

Synthesis and characterization of magnetic nanoparticles of cobalt ferrite coated with silica

Daniely Ferreira de Queiroz ¹, Emerson Rodrigues de Camargo ² , Marco Antonio Utrera Martines ¹ ¹Institute of Chemistry, Federal University of Mato Grosso do Sul, Cidade Universitaria, Campo Grande, MS 79074-460, Brazil²Department of Chemistry, Federal University of São Carlos. Rod. Washington Luis km 235, CP 676 São Carlos SP, 13565-9905. Brazil*corresponding author e-mail address: marco.martines@ufms.br | [6603386498](https://orcid.org/0000-0002-6603-3864)

ABSTRACT

There are several methods available for magnetic nanoparticles (MNP) synthesis, and in this study the coprecipitation method is employed. The cobalt ferrites (CF) were prepared using aqueous solutions of Co^{2+} and Fe^{3+} chloride with a stoichiometry proportion of $\text{Co:Fe} = 1:2$. Thus, the aging temperatures were 27, 27/98, 60, 80 and 98 °C, during which the precipitation occurred at 27 °C and the aging one at 98 °C for the FC27/98 sample. As a result, the study showed that a single crystal phase material was obtained at the aging temperature of 98 °C during 1 h and with a mean particle size of $42 \text{ nm} \pm 7.4 \text{ nm}$ and degree of polydispersity of 18%. The FC98/SiOH coated nanoparticle had a surface area of $11 \text{ m}^2 \text{ g}^{-1}$, saturation magnetization of 10.05 emu g^{-1} a mean particle size of $773.4 \text{ nm} \pm 131.1 \text{ nm}$ and a degree of polydispersity of 17 %. It was possible to confirm that it had a silica coating of cobalt ferrite nanoparticles by DRIFT and EDX indicated the presence of silica.

Keywords: coprecipitation; CoFe_2O_4 ; SiO_2 ; magnetic nanoparticles; nanotechnology

1. INTRODUCTION

Iron oxide nanoparticles[1] and their mixtures [2] have been extensively studied in several areas such as physics [3] chemistry [4], materials science[5], biology [6] and medicine [7] due to their unusual properties [8]. Magnetic nanoparticles became a topic of interest over the last decade because of their applicability in data storage[9], catalysis[10], magnetic paint[11], environmental decontamination[12], microelectronics [13], high-density magnetic recording [14], magnetic refrigeration [15] with therapeutic applications in biomedical [16], cell separation [17] and cancer treatment.

The behaviour of particles in nanoscale [18] as well as their physical [19] and chemical properties are quite different when compared to those observed at macroscopic scale. This is caused by the size reduction that includes confinement effects, dependency between electronic structure and particle size, interface phenomena and effects induced by increasing surface area [20].

New methods have been developed for the synthesis of magnetic nanoparticles through a variety of techniques. Moreover, modifying their surface has been improved their properties, providing new strategies for the production of different materials with potential applications in many fields, such as spintronics system and controlled release of drugs. The development of magnetic nanoparticles that compete for most of these applications, certain considerations must be taken into account such as stability chemical and structural composition of the system shell / core. These characteristics depend on the route of synthesis of the nanoparticles and the methods used to prepare and stabilize

colloidal systems. The nanoparticles of cobalt ferrite (CoFe_2O_4) are remarkably interesting due to its high coercivity [21] moderate saturation magnetization [22], high magnetocrystalline anisotropy [23] and high structural stability at higher temperatures and chemical [24].

There are several routes for the synthesis of magnetic nanoparticles of different sizes, such as water-oil microemulsion [25], microwave processing [26], mechanical grinding [27], reverse micelle [28], combustion [29], co-precipitation [30], pyrolysis [31] and among others. The magnetic core of the magnetic nanoparticles can be coated with a polymeric layer of not active sites or anchoring organic molecules to a metal surface [32]. These particles can be considered as hybrid materials that can be an alternative to production of new multifunctional material. Among the various methods of synthesis, the co-precipitation of iron and cobalt ions in alkaline medium is a method that has presents several advantages, such as relatively low reaction temperature and time, low cost and narrow particle size distribution. Based on considerations of its importance for understanding more intense each step of the synthesis using the method of co-precipitation, the magnetic properties, particle size, surface area, and crystalline phase of these were conducted a systematic investigation on the CoFe_2O_4 based on characteristics of nanoparticles.

The present work shows experimental data to obtain cobalt ferrite according to a study of the influence of aging temperature in the synthesis of magnetic cores and coating of the nanoparticles. Several aging temperatures were studied 98, 80, 60, 27/98 e 27 °C.

2. MATERIALS AND METHODS

2.1. Reagents.

All the reactions were carried out using ultrapure water from a Millipore Ellex system and the chemical reagents were used as received without any treatment or purification. Nanoparticles were synthesized using cobalt (II) chloride hexahydrate

($\text{CoCl}_2 \cdot 6\text{H}_2\text{O}$, 98% Sigma-Aldrich), iron (III) chloride tetrahydrate ($\text{FeCl}_3 \cdot 4\text{H}_2\text{O}$, 98% Sigma-Aldrich), sodium hydroxide (95% Synth), tetraethyl orthosilicate (98% Sigma-Aldrich) and ethanol (98% Sigma-Aldrich).

2.2. Synthesis of cobalt ferrite magnetic nanoparticles.

Stock solutions of cobalt (II) chloride (2.5 mmol L^{-1}), iron (III) chloride (5 mmol L^{-1}) and sodium hydroxide (5 mol L^{-1}) were prepared at room temperature by dissolving their respective salts in ultrapure water. The cobalt ferrite was prepared by means of the co-precipitation method. The solutions were mixed in the stoichiometric ratio of $\text{Co:Fe} = 1:2$ at pH 13 under mechanical agitation at 700 rpm at different temperatures (27, 60, 80 and 98°C). The NaOH solution was used to adjust the pH. The product obtained was aging at the same temperature of co-precipitation under agitation for 1 hour, except for the sample co-precipitate at 27°C that was also aged at 98°C . Furthermore, to remove the excess base, the solid obtained was washed with ultrapure water several times to reach a neutral pH. Finally, the dark solid was dried at 80°C for 24 hours in a stove.

2.3. Coating of cobalt ferrite nanoparticles with silica.

The coating of the nanoparticles was carried out in accordance with the method of Stober [33]. In the representative procedure, 0.11g of ferrite sample synthesized with aging temperature to 98°C (called FC98) was dispersed in 480 mL of ethanol solution: water mixture (molar ratio ethanol: water 1.5:1 v/v) followed by addition of $560 \mu\text{L}$ of 1 mol L^{-1} sodium hydroxide. After this, $240 \mu\text{L}$ of TEOS was added and vigorously stirred in a

magnetic stirrer. The solution was kept for 24 hours at room temperature and the reaction system was partially sealed to prevent evaporation. After this, a further $240 \mu\text{L}$ of TEOS was added and kept for 48 hours at room temperature to complete the coating reaction. The dry material was stored in a sealed glass. The obtained material was encoded as FC98/ SiO_2 .

2.4. Instrumentation and Measurements.

The materials were characterized by X-ray diffraction (XRD) using Cu K α radiation in the 2θ range from 5 to 75° with a step of 0.02° . The surface area was measured through adsorption isotherms of nitrogen at a temperature of 77 K . The chemical composition of the nanoparticles was semiquantitatively evaluated by energy-dispersive X-ray analysis (EDX) and the analysis was conducted by infrared spectroscopy in a Fourier Transform Infrared Spectrometer (FTIR). The nanoparticles were analyzed by means of diffuse reflectance accessory (DRIFT). The morphology of the solid material was investigated by transmission electron microscopy (TEM) using a Philips CM120 microscope operating at 120 kV . The magnetic profile was obtained through a conventional vibrating sample magnetometer (VSM) with fields of 2 T at room temperature.

3. RESULTS

3.1. Synthesis and characterization of magnetic CoFe_2O_4 particles.

Magnetic ferrite CoFe_2O_4 nanoparticles synthesized by the coprecipitation route are formed through a process of dehydration and crystallization.

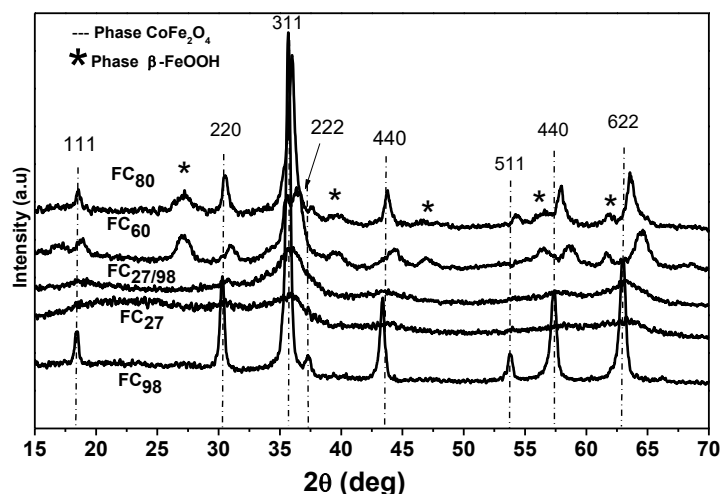
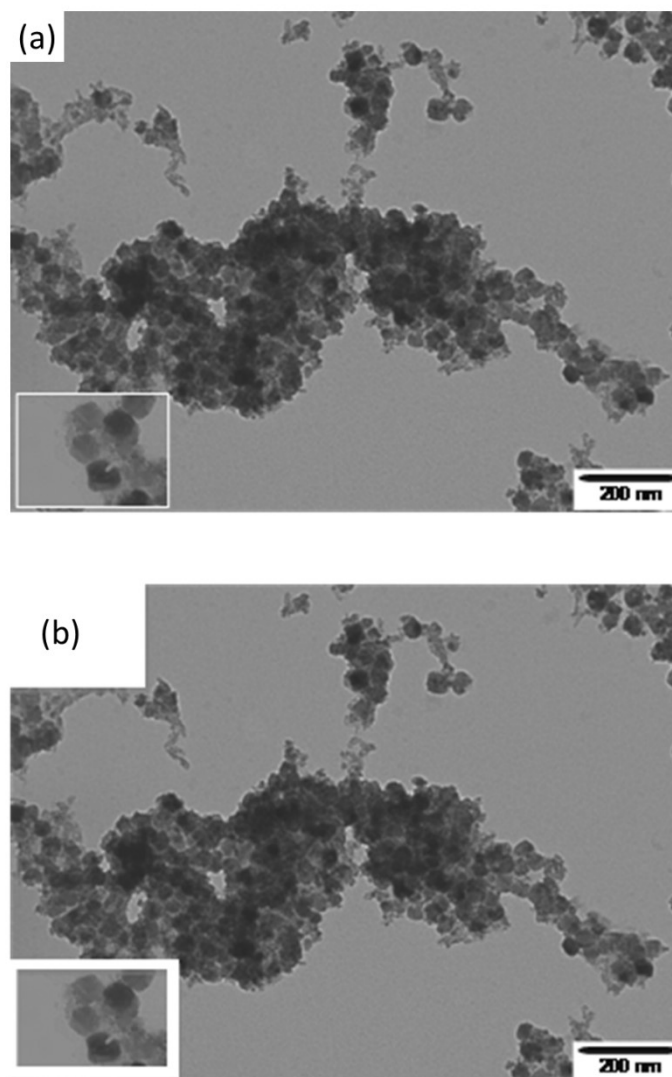


Figure 1. X-ray diffractograms of the samples of cobalt ferrites prepared in different temperatures. FC98 – 98°C , FC27 – 27°C , FC27/98 – 27°C (first stage) e 98°C (second stage), FC60 – 60°C e FC80 – 80°C .

For this reason, an aging period is essential to form these nanoparticles. If the time and aging temperature are controlled, the growth mechanism and phase transformation can be modified, which opens up an opportunity to choose the most suitable morphology and structure of the nanoparticles. On the other hand, the oxyhydroxide crystalline materials, in particular the akaganeite $\beta\text{-FeOOH}$ phase, display a reddish-brown color and have an antiferromagnetic behavior, which means its presence in any material can serve to reduce its magnetic properties.



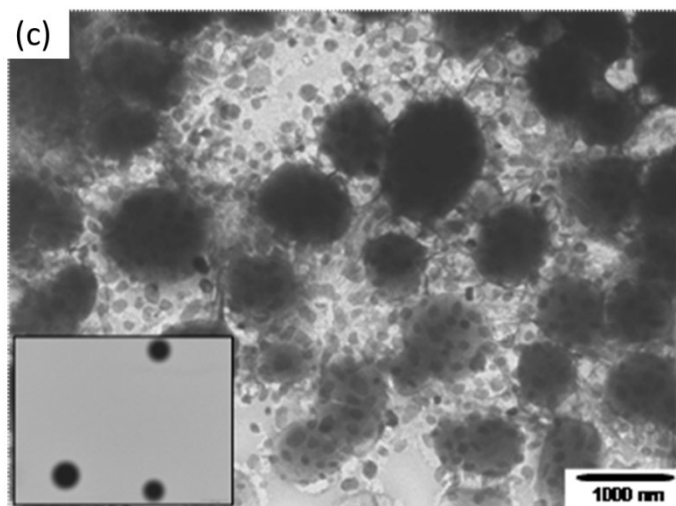


Figure 2. Image of transmission electron microscopy (TEM) of samples, (a) FC98, (b) FC27/98, (c) FC98/SiOH. In all the images shows an enlargement of a part of the micrograph of the corresponding materials, respectively.

As a means of evaluating how the temperature affects the synthesis, the coprecipitated precursors were aged at different temperatures and their respective XRD patterns are shown in Figure 1. Miller indices assign the magnetic CoFe_2O_4 phase (PDF 22-1086) and the (*) symbol indicates the secondary $\beta\text{-FeOOH}$ phase (PDF 29-0712). It is clear that pure CoFe_2O_4 only formed aging in the coprecipitate at the highest temperature of 98°C (FC98) while the akaganeite $\beta\text{-FeOOH}$ phase was present in the materials aged at lower temperatures (FC88 and FC60). Aging at room temperature (FC27) resulted in a nearly amorphous material, with a single broad peak at approximately 35° , which is related to the (311) diffraction peak, even when post-treated at 98°C (FC27/98).

The TEM images of Figure 2 of the FC98, FC27/98 e FC98/SiO₂ samples respectively. Figure 2a features an average particle diameter of approximately $42\text{ nm} \pm 7.4\text{ nm}$ and degree of polydispersity of 18%; Figures 2b, and 2c feature an average particle diameter of approximately $31.2\text{ nm} \pm 7.0\text{ nm}$ and degree of polydispersity of 22% and $773.4\text{ nm} \pm 131,1\text{ nm}$ and degree of polydispersity 17 %, respectively. The degree of polydispersity can be calculated from the ratio between the standard deviation and the average particle diameter.

The magnetic profile of FC98, FC27/98 and FC98/SiOH showed the typical behavior of ferrimagnetic material, as can be observed in Figure 3 a, b e c respectively; there was a hysteresis loop in the material which shows saturation magnetization values of 39.7, 27.48 and 10.05 emu g^{-1} respectively. The ferromagnetic materials display a magnetic memory field caused by the presence of magnetization remaining i.e.it is necessary to return to the initial magnetization, there is an application of a magnetic field in the opposite direction. The main advantage of these systems is that they provide the magnetic recording where the recorded information is preserved, even when there is no electricity present.

3.2. Coating of magnetic nanoparticles of CoFe_2O_4 .

The purpose of coating the magnetic nanoparticles is to allow the isolation and encapsulation of these materials and thus avoid problems such as oxidation; moreover, it improves the degree of biocompatibility when they are used in biological

systems. A FC98/SiO₂ submitted a surface area of $11.21 \pm 0.15\text{ m}^2\text{ g}^{-1}$, because the silica coating of the surface area had decreased by 78%, compared with the surface area of cobalt ferrite before it was coated with silica.

With regard to the magnetic measurement of the sample FC98/SiO₂, as can be seen in Figure 3c, the hysteresis loop of the material displays saturation magnetization. This magnetic profile can be seen in the graph of Magnetization versus the Applied Magnetic Field and shows the typical behavior of the ferrimagnetic material. The measured magnetization is in accordance with the data provided by XRD.

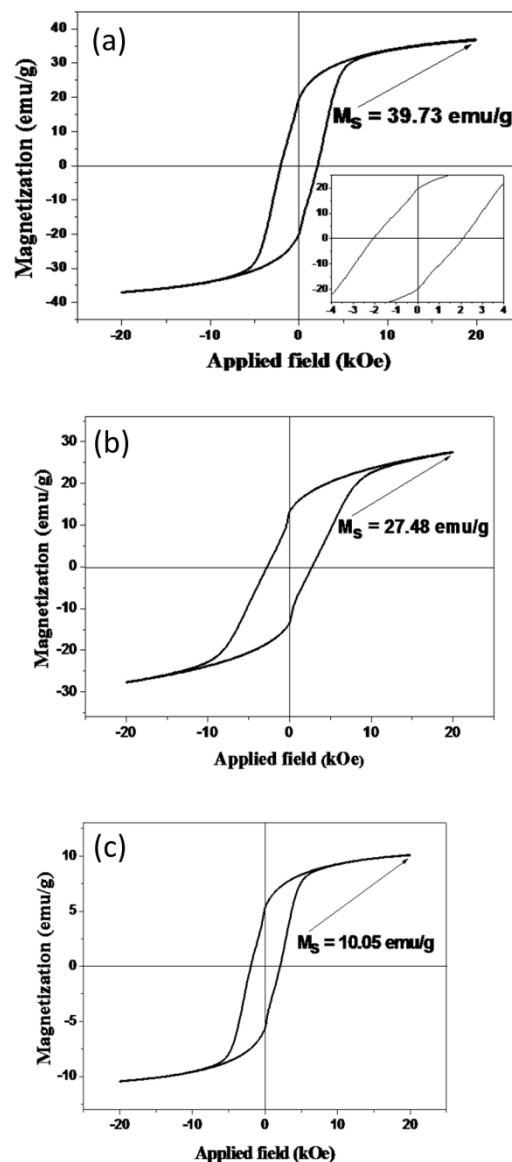


Figure 3. Magnetic hysteresis and its respective saturation magnetization (M_s) for the sample (a) FC98, (b) FC27/98 and (c) FC98/SiOH respectively, which is subject to a magnetic field of 20 kOe.

Although the magnetic nanoparticles maintained their ferromagnetic character (magnetic core), there was reduced saturation magnetization owing to the thickness of the silica layer covering the magnetic core (CoFe_2O_4) which in the case of diamagnetic material, tends to reduce the magnetization of the material. In Figure 4, there is a DRIFTS spectrum of the samples of silica, ferrite, cobalt ferrite and silica coated with uncoated cobalt. It can be determined that before being recoated with silica, the cobalt ferrite has vibrational modes in the region of 570 cm^{-1}

and 632 cm^{-1} which are characteristic of cobalt ferrite. The FC98/SiO₂ sample has vibrational modes with asymmetric stretching absorption in the region $900\text{--}1200\text{ cm}^{-1}$ associated with the Si-OH and O-Si-O groups, thus indicating the presence of silica. The coating was also analyzed semi-quantitatively for the FC98/SiOH sample by means of the energy dispersive spectroscopy X-ray (EDX) technique which had an average molar composition of 66.51% Si, 22.68% Fe and 11.14% Co.

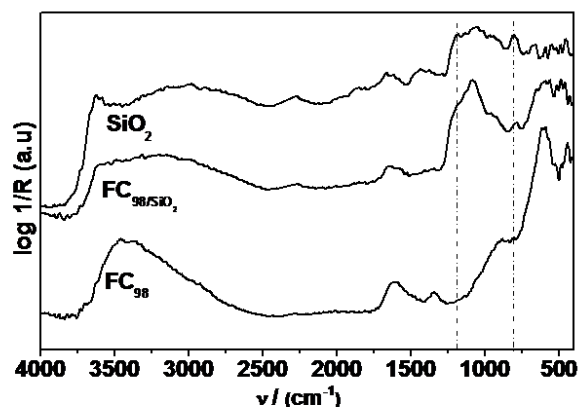


Figure 4. Infrared spectrum diffuse reflectance Fourier transform (DRIFT) samples of uncoated cobalt ferrite FC98, silica and pure cobalt ferrite coated with silica FC98/SiO₂.

3.3. Testing for kinetic or thermodynamic influences on the synthesis of cobalt ferrite.

Three replications of the methodology were employed to study the reproducibility of the synthesis of FC98 and FC27/98; these were also carried out to study the nature of the aging time, or the reaction product of a property that is dependent on kinetics or thermodynamics. Tests were performed by employing the FC98 methodology and the sample was subjected to an aging time of 5

minutes at $98\text{ }^{\circ}\text{C}$ and included a mixture of CoFe₂O₄ phases with the oxyhydroxide phase; in addition, it was noted that five minutes was not enough time to form a single crystalline phase.

It was also found that this material showed no magnetic properties. Another test was conducted by employing the methodology required for the synthesis of FC60 when conditioned for a minimum aging period of 24 hours. This sample only showed a crystalline phase of CoFe₂O₄ and we observed that this material has magnetic properties. When these data are compared, it can be concluded that the crystalline phase of cobalt ferrite is dependent on a kinetic process and this fact can be observed in the XRD in Figure 5.

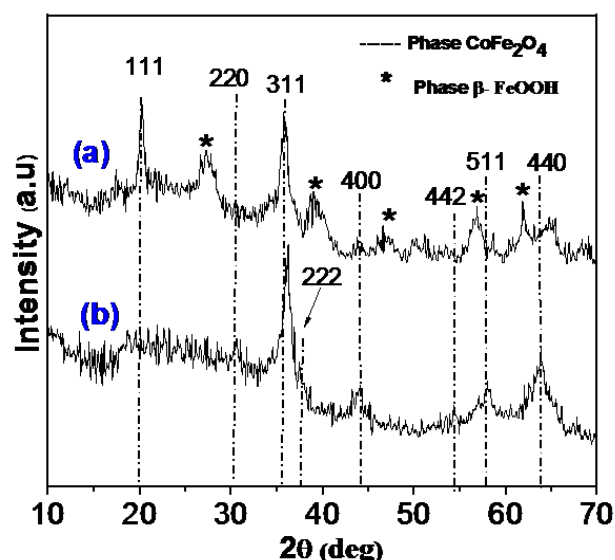


Figure 5. X-ray diffractograms of samples of cobalt ferrite (thermodynamic or kinetic testing), (a) synthesis of FC98 with aging time of 5 minutes at a temperature of $98\text{ }^{\circ}\text{C}$, (b) synthesis (FC60) with aging time of 24 hours at a temperature $60\text{ }^{\circ}\text{C}$.

4. CONCLUSIONS

This paper investigates the influence of aging temperature on the synthesis of magnetic cobalt ferrite coating with silica. Several aging temperatures were studied such as 98, 80, 60, 27/98 and $27\text{ }^{\circ}\text{C}$. The aging temperature of 98 and $27/98\text{ }^{\circ}\text{C}$ showed the best conditions for preparing a single phase of cobalt ferrite, CoFe₂O₄, with a particle size of less than 100 nm. It was observed that a rise in temperature aging led to a significant increase in saturation magnetization and remanence factors for their magnetic properties. Some parameters are kept fixed for the synthesis that is required for obtaining the cobalt ferrites such as the following: final pH of the reaction equal to 13, while the aging temperature covered a period of 1 hour, and the concentration of base 5 mol L^{-1} solution sodium hydroxide. It was possible to obtain a single phase of cobalt ferrite (FC98) that had a particle size of $42\text{ nm} \pm 7.4\text{ nm}$ and a polydispersity of 18%, saturation magnetization of 39.7 emu g^{-1} . The sample FC98 was selected because it presented single

cobalt ferrite phase for the silica coating. The shell / core type coating system (FC98/SiOH) had a surface area of $11.21 \pm 0.15\text{ m}^2\text{ g}^{-1}$, the mean particle size of $773.4\text{ nm} \pm 131.1\text{ nm}$ and a degree of polydispersity of 17%. The particles covered with silica presented saturation magnetization 10.05 emu g^{-1} and. The nanoparticle cobalt ferrite coating system (FC98/SiOH) was characterized using the DRIFT technique, which presented vibrational modes with asymmetric stretching absorption in the region $900\text{--}1200\text{ cm}^{-1}$ associated with the Si-OH and O-Si-O groups, thus indicating the presence of silica in the particle surface.

Therefore, the parameters studied and obtained in this work, the nanoparticle of cobalt ferrite, as well as cobalt ferrite coating with silica showed with ferrimagnetic properties, with the possibility of applying this material to the data storage by magnetic memory.

5. REFERENCES

1. Prabhu, P.; Patravale, V. The Upcoming Field of Theranostic Nanomedicine: An Overview. *J. Biomed. Nanotechnol.* **2012**, *8*, 859-882, <https://doi.org/10.1166/jbn.2012.1459>.
2. Sharifi, S.; Behzadi, S.; Laurent, S.; Forrest, M.L.; Stroeve, P.; Mahmoudi, M. Toxicity of nanomaterials. *Chem. Soc. Rev.* **2012**, *41*, 2323-2343, <https://doi.org/10.1039/C1CS15188F>.
3. Queiroz, D.F.; Dadamos, T.R.L.; Machado, S.A.S.; Martinez, M.A.U. Electrochemical Determination of Norepinephrine by

Means of Modified Glassy Carbon Electrodes with Carbon Nanotubes and Magnetic Nanoparticles of Cobalt Ferrite. *Sensors* **2018**, *18*, 1223-1234, <https://doi.org/10.3390/s18041223>.

4. Akbari, A.; Arsalani, N.; Eftekhari-Sis, B.; Amini, M.; Gohari, G.; Jabbari, E. Cube-octameric silsesquioxane (POSS)-capped magnetic iron oxide nanoparticles for the efficient removal of methylene blue. *Frontiers of Chemical Science and Engineering*. **2019**, *13*, 563-573, <https://doi.org/10.1007/s11705-018-1784-x>.

5. Clavijo-Jordan, V.; Kodibagkar, V.D.; Beeman, S.W.C.; Hann, B.D.; Bennett, K.M. Principles and emerging applications of nanomagnetic materials in medicine. *Rev.-Nanomed. Nanobiotechnol.* **2012**, *4* 345-365, <https://doi.org/10.1002/wnan.1169>.

6. Irshad, R.; Tahir, K.; Li, B.; Ahmad, A.; Siddiqui, A.R.; Nazir, S. Antibacterial activity of biochemically capped iron oxide nanoparticles: A view towards green chemistry. *J. Photoch. Photobio. B* **2017**, *170*, 241-246, <https://doi.org/10.1016/j.jphotobiol.2017.04.020>.

7. Mok, H.; Zhang, M.Q. Superparamagnetic iron oxide nanoparticle-based delivery systems for biotherapeutics. *Expert Opin. Drug Deliv.* **2013**, *10*, 73-87, <https://doi.org/10.1517/17425247.2013.747507>.

8. Qin, F.X.; Peng, H.X. Ferromagnetic microwires enabled multifunctional composite materials *Prog. Mater. Sci.* **2013**, *58*, 183-259, <https://doi.org/10.1016/j.pmatsci.2012.06.001>.

9. Zhu, N.; Ji, H.; Yu, P.; Niu, J.; Farooq, M.U.; Akram, M.W.; Udego, I.O.; Li, H.; Niu, X. Surface Modification of Magnetic Iron Oxide Nanoparticles. *Nanomaterials* **2018**, *8*, 810-838, <https://doi.org/10.3390/nano8100810>.

10. Baig, R.B.N.; Varma, R.S. Magnetically retrievable catalysts for organic synthesis. *Chem. Commun.* **2013**, *49*, 752-770, <https://doi.org/10.1039/C2CC35663E>.

11. Siddiqui, K.S.; Rahman, A.; Husen, A. Biogenic Fabrication of Iron/Iron Oxide Nanoparticles and Their Application *Nanoscale Res Lett.* **2016**, *11*, 498-510, <https://doi.org/10.1186/s11671-016-1714-0>.

12. Song, J.; Zhang, F.; Huang, Y.; Keller, A.A.; Tang, X.; Zhang, W.; Jiaf, W.; Santos, J. Highly efficient bacterial removal and disinfection by magnetic barium phosphate nanoflakes with embedded iron oxide nanoparticles. *Environmental Science: Nano* **2018**, *5*, 1341-1349, <https://doi.org/10.1039/C8EN00403J>.

13. Oh, Y.; Choi, C.; Hong, D.; Kong, S.D.; Jin, S. Magnetically Guided Nano-Micro Shaping and Slicing of Silicon. *Nano Lett.* **2012**, *12*, 2045-2050, <https://doi.org/10.1021/nl300141k>.

14. Rawat, R.S. High Energy Density Pulsed Plasmas in Plasma Focus: Novel Plasma Processing Tool for Nanophase Hard Magnetic Material Synthesis. *Nanosci. Nanotechnol. Lett.* **2012**, *4*, 251-274, <https://doi.org/10.1166/nnl.2012.1318>.

15. Yamamoto, T.; Shull, R.D.; Bandaru, P.R.; Cosandey, F.; Hahn, H.W. Superparamagnetic nanocomposite of silver iron-oxide by inert-gas condensation. *Jpn. J. Appl. Phys. Part 2-Lett.* **1994**, *33*, 1301-1303, <https://doi.org/10.1143/JJAP.33.L1301>.

16. Cheraghipour, E.; Tamaddon, A.M.; Javadpour, S.; Bruce, I.J. PEG conjugated citrate-capped magnetite nanoparticles for biomedical applications. *J. Magn. Magn. Mater.* **2013**, *328*, 91-95, <https://doi.org/10.1016/j.jmmm.2012.09.042>.

17. Zhao, L.; Chano, T.; Morikawa, S.; Saito, Y.; Shiino, A.; Shimizu, S.; Maeda, T.; Irie, T.; Aonuma, S.; Okabe, H.; Kimura, T.; Inubushi, T.; Komatsu, N. Hyperbranched Polyglycerol-Grafted Superparamagnetic Iron Oxide Nanoparticles: Synthesis, Characterization, Functionalization, Size Separation, Magnetic Properties, and Biological Applications. *Adv. Funct. Mater.* **2012**, *22*, 5107-5117, <https://doi.org/10.1002/adfm.201201060>.

18. Wang, Y.L.; Irudayaraj, J. Surface-enhanced Raman spectroscopy at single-molecule scale and its implications in biology. *Philos. Trans. R. Soc. B-Biol. Sci.* **2013**, *368*, 20026-20034, <https://doi.org/10.1098/rstb.2012.0026>.

19. Gagner, J.E.; Qian, X.; Lopez, M.M.; Dordick, J.S.; Siegel, R.W. Effect of gold nanoparticle structure on the conformation and function of adsorbed proteins. *Biomaterials* **2012**, *33*, 8503-8516, <https://doi.org/10.1016/j.biomaterials.2012.07.009>.

20. Palanisamy, S.; Wang Y.M. Superparamagnetic iron oxide nanoparticulate system: synthesis, targeting, drug delivery and therapy in cancer. *Dalton Transactions* **2019**, *26*, 9490-9515, <https://doi.org/10.1039/c9dt00459a>.

21. Rafique, M.Y.; Pan, L.Q.; Javed, Q.U.A.; Iqbal, M.Z.; Yang, L.H. Influence of NaBH₄ on the size, composition, and magnetic properties of CoFe₂O₄ nanoparticles synthesized by hydrothermal method. *J. Nanopart. Res.* **2012**, *14*, 1189-1196, <https://doi.org/10.1007/s11051-012-1189-6>.

22. Cao, D.; Li, H.; Pan, L.; Li, J.; Wang, X.; Jing, P.; Cheng, X.; Wang, W.; Wang, J.; Liu, Q. High saturation magnetization of γ -Fe₂O₃ nano-particles by a facile one-step synthesis approach. *Sci. Rep.* **2013**, *6*, 32360-32368, <https://doi.org/10.1038/srep32360>.

23. Maldonado-Camargo, L.; Unni, M.; Rinaldi, C. Magnetic Characterization of Iron Oxide Nanoparticles for Biomedical Applications. *Methods Mol Biol.* **2017**, *1570*, 47-71, https://doi.org/10.1007/978-1-4939-6840-4_4.

24. Sujatha, C.; Reddy, K.V.; Babu, K.S.; Reddy, A.R.; Rao, K.H. Effects of heat treatment conditions on the structural and magnetic properties of MgCuZn nano ferrite. *Ceram. Int.* **2012**, *38*, 5813-5820, <https://doi.org/10.1016/j.ceramint.2012.04.029>.

25. Solla-Gullon, J.; Gomez, E.; Valles, E.; Aldaz, A.; Feliu, J.M. Synthesis and structural, magnetic and electrochemical characterization of PtCo nanoparticles prepared by water-in-oil microemulsion. *J. Nanopart. Res.* **2010**, *12*, 1149-1154, <https://doi.org/10.1007/s11051-009-9680-4>.

26. Aivazoglou, E.; Metaxa, E.; Hristoforou, E. Microwave-assisted synthesis of iron oxide nanoparticles in biocompatible organic environment. *AIP Advances* **2018**, *8*, 0482011-04820114, <https://doi.org/10.1063/1.4994057>.

27. Can, H.K.; Kavlak, S.; ParviziKhosroshahi, S.; Güner, A. Preparation, characterization and dynamical mechanical properties of dextran-coated iron oxide nanoparticles (DIONPs). *Artificial Cells, Nanomedicine, and Biotechnology An International Journal* **2018**, *46*, 421-431, <https://doi.org/10.1080/21691401.2017.1315428>.

28. Wang, C.L.J.; Wu, Y.M.A.; Jacobs, R.M.J.; Warner, J.H.; Williams, G.R.; O'Hare, D. Reverse Micelle Synthesis of Co-Al LDHs: Control of Particle Size and Magnetic Properties. *Chem. Mater.* **2011**, *23*, 171-180, <https://doi.org/10.1021/cm1024603>.

29. Kamboja, N.; Shamshirgar, S.A.; Shirshneva-Vaschenko, E.V.; Hussainova, I. Deposition of iron oxide nanoparticles on mesoporous alumina network by wet-combustion technology. *Mater. Chem. Phys.* **2019**, *225*, 340-346, <https://doi.org/10.1016/j.matchemphys.2018.12.095>.

30. LaGrow, A.P.; Besenhard, M.O.; Hodzic, A.; Sergides, A.; Bogart, L.K.; Gavriilidis, A.; Thanh, N.T.K. Unravelling the growth mechanism of the co-precipitation of iron oxide nanoparticles with the aid of synchrotron X-Ray diffraction in solution. *Nanoscale* **2019**, *11*, 6620-6628, <https://doi.org/10.1039/C9NR00531E>.

31. Din, M.I.; Raza, M.; Hussain, Z.; Mehmood, H.A. Fabrication of magnetite nanoparticles (Fe₃O₄-NPs) for catalytic pyrolysis of nutshells biomass. *J. Soft Mater.* **2019**, *17*, 24-31, <https://doi.org/10.1080/1539445X.2018.1542315>.

32. Drost, M.; Tu, F.; Berger, L.; Preischl, C.; Zhou, W.; Gliemann, H.; Wöll, C.; Marbach, H. Surface-Anchored Metal–Organic Frameworks as Versatile Resists for Gas-Assisted E-

Beam Lithography: Fabrication of Sub-10 Nanometer Structures. *ACS Nano* **2018**, 12, 3825-3835, <https://doi.org/10.1021/acsnano.8b01071>.

33. Stöber, W.; Fink, A.; Bohn, E. Controlled growth of monodisperse silica spheres in the micron size range *J. Colloid Interface Sci.* **1968**, 26, 62-69, [https://doi.org/10.1016/0021-9797\(68\)90272-5](https://doi.org/10.1016/0021-9797(68)90272-5).

6. ACKNOWLEDGEMENTS

The authors would like to thank the Universidade Federal de Mato Grosso do Sul. This study was financed in part by the Coordenação de Aperfeiçoamento de Pessoal de Nível Superior – Brasil (CAPES) – Finance Code 001. The authors are also grateful to the Conselho Nacional de Desenvolvimento Científico e Tecnológico - Brasil (CNPq) - Finance Code 408054/2013-1 and Fundação de Apoio ao Desenvolvimento do Ensino, Ciência e Tecnologia do Estado de Mato Grosso do Sul – Brasil (FUNDECT-MS) – grants 112/2014 for providing financial support for undertaking this project. The fellowship provided to D.F.Q. by CAPES (Coordenação de Aperfeiçoamento de Pessoal de Nível Superior) is also greatly appreciated.



© 2019 by the authors. This article is an open access article distributed under the terms and conditions of the Creative Commons Attribution (CC BY) license (<http://creativecommons.org/licenses/by/4.0/>).